Article

Photocatalytic Water Splitting for Hydrogen Production with Novel Y_2MSbO_7 (M = Ga, In, Gd) under Visible Light Irradiation

Jingfei Luan * and Jianhui Chen

State Key Laboratory of Pollution Control and Resource Reuse, School of the Environment, Nanjing University, Nanjing 210093, China; E-Mail: jhchenj@gmail.com

* Author to whom correspondence should be addressed; E-Mail: jfluan@nju.edu.cn;
Tel.: +86-(0)-13585206718; Fax: +86-(0)-25-83707304.

Abstract: Novel photocatalysts Y_2MSbO_7 (M = Ga, In, Gd) were synthesized by the solid state reaction method for the first time. A comparative study on the structural and photocatalytic properties of Y_2MSbO_7 (M = Ga, In, Gd) was reported. The results showed that Y_2GaSbO_7, Y_2InSbO_7 and Y_2GdSbO_7 crystallized with the pyrochlore-type structure, cubic crystal system, and space group *Fd3m*. The lattice parameter for Y_2GaSbO_7 was 10.17981 Å. The lattice parameter for Y_2InSbO_7 was 10.43213 Å. The lattice parameter for Y_2GdSbO_7 was 10.50704 Å. The band gap of Y_2GaSbO_7 was estimated to be 2.245 eV. The band gap of Y_2InSbO_7 was 2.618 eV. The band gap of Y_2GdSbO_7 was 2.437 eV. For the photocatalytic water-splitting reaction, H_2 or O_2 evolution was observed from pure water with Y_2GaSbO_7, Y_2InSbO_7 or Y_2GdSbO_7 as catalyst under visible light irradiation. (Wavelength > 420 nm). Furthermore, H_2 and O_2 were also evolved by using Y_2GaSbO_7, Y_2InSbO_7 or Y_2GdSbO_7 as a catalyst from CH_3OH/H_2O and $AgNO_3/H_2O$ solutions, respectively, under visible light irradiation (λ > 420 nm). Y_2GaSbO_7 showed the highest activity compared with Y_2InSbO_7 or Y_2GdSbO_7. At the same time, Y_2InSbO_7 showed higher activity compared with Y_2GdSbO_7. The photocatalytic activities were further improved under visible light irradiation with Y_2GaSbO_7, Y_2InSbO_7 or Y_2GdSbO_7 being loaded by Pt, NiO or RuO_2. The effect of Pt was better than that of NiO or RuO_2 for improving the photocatalytic activity of Y_2GaSbO_7, Y_2InSbO_7 or Y_2GdSbO_7.

1. Introduction

Since water splitting which was catalyzed by TiO_2 was discovered in 1972 [1], photocatalysis had attracted large-scale attention from both academic and industrial organizations [2–6]. In particular, water splitting by the photocatalytic method had been regarded as a highly promising process to acquire a clean and renewable H_2 source [5–13]. Presently, TiO_2 is the most common photocatalyst for water splitting, but TiO_2 cannot be utilized in the visible light region and can only split water under ultraviolet light irradiation. In addition, ultraviolet light only occupies 4% of sunlight, which is a limitative factor for photocatalytic technology with TiO_2 as the catalyst. Thus, some efficient catalysts which can produce electron–hole pairs under visible light irradiation should be developed because visible light occupies 43% of sunlight.

Fortunately, $A_2B_2O_7$ compounds are often considered as possessing excellent photocatalytic properties under visible light irradiation [14,15]. In our previous work [14], we had found that Bi_2GaVO_7 crystallized with the tetragonal crystal system and could split pure water into hydrogen under ultraviolet light irradiation and seemed to have potential for improvement of photocatalytic activity by modification of its structure. Based on the above analysis, we could deduce that the substitution of Bi^{3+} by Y^{3+}, and the substitution of Ga^{3+} by In^{3+} or Gd^{3+}, and the substitution of V^{5+} by Sb^{5+} in Bi_2GaVO_7, might promote carriers concentration. The substitution will result in the lattice O^{2-} and O^- ionosorbed on the surface, which can enhance the photocatalytic activity of solid-solution photocatalysts [16]. Besides these reasons, we believe the substitution can form the impurity energy levels in the band gap of these catalysts or create band gap narrowing. As a result, some impurity energy levels or narrow band gap which own low band gap energy will promote carrier concentration. With the lower band gap energy or the impurity energy level, light energy will be easy to be larger than above energy and more electrons and holes will be easy to be produced, thus the substitution might promote carriers concentration. Borse *et al.* converted the visible-light-inactive $BaSnO_3$ into a v isible-light-active photocatalyst for O_2 production via the electronic structure tuning by substituting Pb for Sn [17]. Yi *et al.* tuned the electronic structure of $NaTaO_3$ by partial substitution of Na with La and Ta with Co. the results show that the absorption edge of $NaTaO_3$ can be extended gradually to the visible-light region, thus resulting in the photocatalytic H_2 production under visible light irradiation [18]. The above results show that the substitution can promote carriers concentration. As a result, a change and improvement of the electrical transportation and photophysical properties could be found in the novel Y_2GaSbO_7, Y_2InSbO_7 or Y_2GdSbO_7 compound, which may possess excellent photocatalytic properties.

Y_2GaSbO_7, Y_2InSbO_7 or Y_2GdSbO_7 have never been produced and the data about their structural and photophysical properties such as space group and lattice constants have not yet been found. Moreover, the photocatalytic properties of Y_2GaSbO_7, Y_2InSbO_7 or Y_2GdSbO_7 have not been investigated by other researchers. The molecular composition of Y_2GaSbO_7, Y_2InSbO_7 or Y_2GdSbO_7

is very similar to other $A_2B_2O_7$ compounds. Thus, the resemblance suggests that Y_2GaSbO_7, Y_2InSbO_7 or Y_2GdSbO_7 could own photocatalytic properties under visible light irradiation, which is similar with those other members in $A_2B_2O_7$ family. Y_2GaSbO_7, Y_2InSbO_7 or Y_2GdSbO_7 also seem to bear potential for improvement of photocatalytic activity by modification of their structure because it has been proved that a slight modification of a semiconductor structure would lead to a tremendous change in photocatalytic properties [19].

In this paper, a novel semiconductor compound Y_2GaSbO_7, Y_2InSbO_7 or Y_2GdSbO_7 was utilized as photocatalyst for splitting water into hydrogen under visible light irradiation. The structural, photophysical and photocatalytic properties of Y_2GaSbO_7, Y_2InSbO_7 or Y_2GdSbO_7 were studied in detail.

2. Experimental

The novel photocatalysts were synthesized by a solid-state reaction method. Y_2O_3, In_2O_3, Gd_2O_3, Ga_2O_3 and Sb_2O_5 with purity of 99.99% (Sinopharm Group Chemical Reagent Co., Ltd., Shanghai, China) were used as starting materials. All powders were dried at 200 °C for 4 h before synthesis. In order to synthesize Y_2GaSbO_7, Y_2InSbO_7 or Y_2GdSbO_7, the precursors were stoichiometrically mixed, then pressed into small columns and put into an alumina crucible (Shenyang Crucible Co., Ltd., China). Ultimately, calcination was carried out at 1320 °C for 65 h in an electric furnace (KSL 1700X, Hefei Kejing Materials Technology CO., Ltd., China). The heating rate of calcination is 0.24 °C/s. The crystal structure of Y_2GaSbO_7, Y_2InSbO_7 or Y_2GdSbO_7 was analyzed by the powder X-ray diffraction method (D/MAX-RB, Rigaku Corporation, Japan) with Cu*K*α radiation (λ = 1.54056). The voltage was 40.0 kV and current was 30.0 mA. The data were collected at 295 K with a step-scan procedure in the range of 2θ = 10°–100°. The step interval was 0.02° and the time per step was 1.2 s. The chemical composition of Y_2GaSbO_7, Y_2InSbO_7 or Y_2GdSbO_7 was determined by scanning electron microscope-X-ray energy dispersion spectrum (SEM-EDS, LEO 1530VP, LEO Corporation, Germany. The scanning accelerating voltage was 20 kV and linked with an Oxford Instruments X-ray analysis system) and X-ray fluorescence spectrometer (XFS, ARL-9800, ARL Corporation, Switzerland). The diffuse reflectance spectra of Y_2GaSbO_7, Y_2InSbO_7 or Y_2GdSbO_7 was analyzed with an UV-visible spectrophotometer (Lambda 40, Perkin-Elmer Corporation, USA) in a UV-Vis diffuse reflectance experiment by the dry-pressed disk samples and $BaSO_4$ was used as the reference material. The surface area of Y_2GaSbO_7, Y_2InSbO_7 or Y_2GdSbO_7 was measured by the Brunauer-Emmett-Teller (BET) method (MS-21, Quantachrome Instruments Corporation, USA) with N_2 adsorption at liquid nitrogen temperature. All the samples were degassed at 180 °C for 8 h prior to nitrogen adsorption measurements. The BET surface area was determined by a multipoint BET method using the adsorption data in the relative pressure (P/P$_0$) range of 0.05–0.3. A desorption isotherm was used to determine the pore size distribution by the Barret-Joyner-Halender (BJH) method, assuming a cylindrical pore model (26). The nitrogen adsorption volume at the relative pressure (P/P$_0$) of 0.994 was used to determine the pore volume and average pore size.

The photocatalytic water splitting was conducted under visible light irradiation in a gas closed circulation system with an inner-irradiation type reactor (quartz cell). A light source (300 W Xe arc lamp, Beijing Dongsheng Glass Light Source Factory, China) with the incident photon flux I_0 of 0.056176 μmol cm^{-2} s^{-1} was focused through a shutter window and a 420 nm cut-off filter onto the

window face of the cell. The gases evolved were determined with a TCD gas chromatogragh (6890 N, Agilent Technologies, USA), which was connected to the gas closed circulation system. 1.0 g catalyst was suspended in 300 mL H_2O under stirrer. Before reaction, the closed gas circulation system and the reaction cell were degassed until O_2 and N_2 could not be detected. Then about 35 Torr of Argon was charged into the system. H_2 evolution reaction was carried out in CH_3OH/H_2O solution (50 mL CH_3OH, 300 mL H_2O) with Pt, NiO or RuO_2-loaded powder as the catalyst.
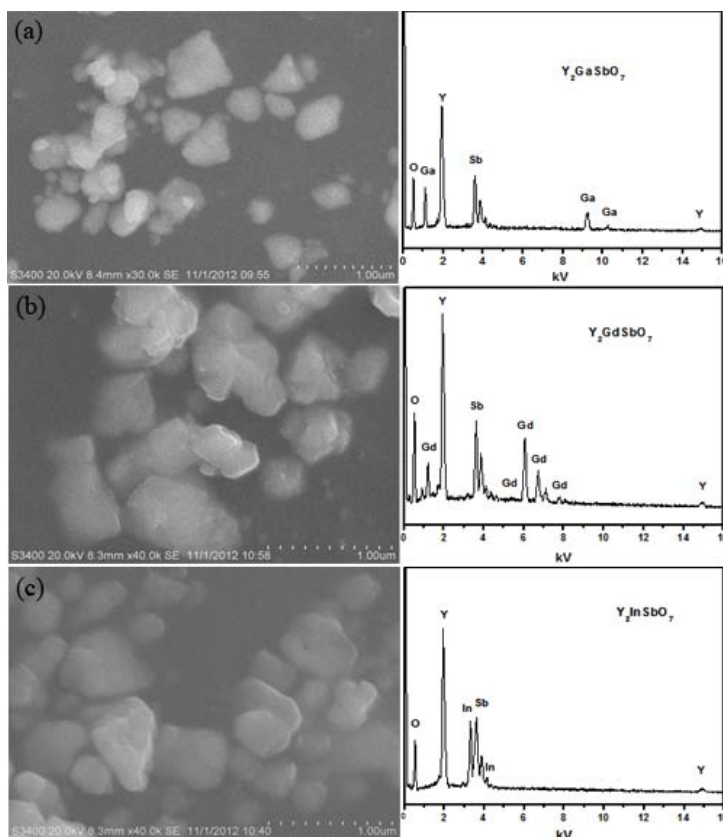
For H_2 evolution reaction, Pt, NiO or RuO_2, which was loaded on the surface of the catalysts, were prepared. Pt was loaded on the catalyst surface by an *in situ* photodeposition method by using aqueous H_2PtCl_6 solution (Shanghai Chemical Reagent Research Institute, China) as the Pt source. NiO or RuO_2, which was loaded on the surface of the catalysts, were prepared by the impregnation method by using $Ni(NO_3)_2$ or $RuCl_3$ solution (Sinopharm Group Chemical Reagent Co., Ltd., Shanghai, China), separately.

3. Results and Discussion

3.1. Characterization

Figure 1 shows the SEM-EDS of Y_2GaSbO_7, Y_2GdSbO_7 and Y_2InSbO_7. Figure 1a–c is for Y_2GaSbO_7, Y_2GdSbO_7 or Y_2InSbO_7. Y_2GaSbO_7, Y_2InSbO_7 or Y_2GdSbO_7 were nanosized particles which owned irregular round shapes.

Figure 1. Scanning electron microscope-X-ray energy dispersion spectrum (SEM-EDS) of (**a**) Y_2GaSbO_7; (**b**)Y_2GdSbO_7 or (**c**) Y_2InSbO_7 prepared by a solid-state reaction method at 1320 °C.

It could be seen from the results that the average particle size of Y_2GaSbO_7 was smaller than that of Y_2InSbO_7 or Y_2GdSbO_7. SEM-EDS spectrum, which was taken from the prepared Y_2GaSbO_7, displayed the presence of yttrium, gallium, antimony and oxygen. Similarly, SEM-EDS spectrum, which was taken from the prepared Y_2InSbO_7, also indicated the presence of yttrium, indium, antimony and oxygen. SEM-EDS spectrum, which was taken from the prepared Y_2GdSbO_7, also indicated the presence of yttrium, gadolinium, antimony and oxygen. Other elements could not be identified from Y_2GaSbO_7, Y_2InSbO_7 or Y_2GdSbO_7.

Figure 2 shows the X-ray powder diffraction patterns of Y_2GaSbO_7, Y_2InSbO_7 and Y_2GdSbO_7. It could be seen from Figure 2 that Y_2GaSbO_7, Y_2InSbO_7 or Y_2GdSbO_7 is a single phase. The calculations of lattice parameters were performed with the program of Cambridge serial total energy package (CASTEP) and first-principles simulation. The CASTEP package is provided by Materials Studio and the CASTEP calculation is composed of the plane-wave pseudopotential total energy method according to the density functional theory. Thus, our calculations are based on the plane-wave-based density functional theory (DFT) in generalized gradient approximations (GGA) with Perdew–Burke–Ernzerh of (PBE) exchange-correlation potential.

Figure 2. X-ray powder diffraction pattern of Y_2GaSbO_7, Y_2InSbO_7 or Y_2GdSbO_7 prepared by a solid-state reaction method at 1320 °C.
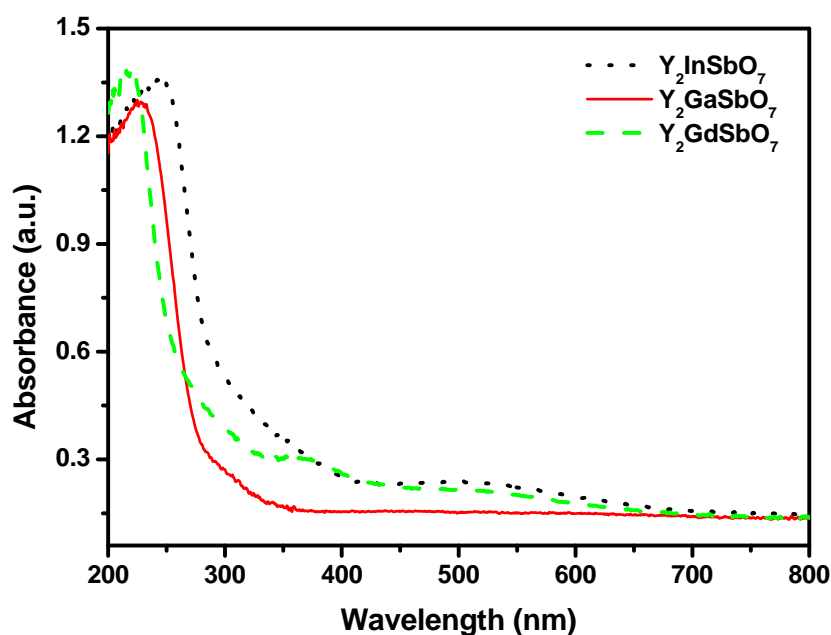

In order to obtain the crystal lattice parameters, Rietveld refinement from XRD data was performed with DBWS, experimental XRD data and simulation XRD data. The uncertainty of the refined lattice parameters are the estimated standard deviation (e.s.d.s), calculated by the full pattern fitting program. However, e.s.d.s are measures of precision rather than of accuracy, and these two terms must not be confused. For a sound estimation of the measurement uncertainty of lattice parameters that are refined from XRD data, more information is needed than just the e.s.d.s that are provided by the Rietveld refinement of the diffraction pattern of the sample. The outcome of refinements for Y_2InSbO_7

generated the unweighted R factors, Rp = 15.28% with space group *Fd3m*. As for Y_2GdSbO_7, Rp was 9.58% with space group *Fd3m*. As for Y_2GaSbO_7, Rp was 12.36% with space group *Fd3m*. According to the Rietveld analysis, Y_2GaSbO_7, Y_2InSbO_7 or Y_2GdSbO_7 owns the pyrochlore-type structure and a cubic crystal system which have a space group *Fd3m*. The lattice parameter for Y_2GaSbO_7 is 10.17981 Å. The lattice parameter for Y_2InSbO_7 is 10.43213 Å and that for Y_2GdSbO_7 is 10.50704 Å. Moreover, the XRD results show that 2 theta angles of each reflection of Y_2GaSbO_7 changed with Ga^{3+} being substituted by In^{3+} or Gd^{3+}. The lattice parameter α increases from $\alpha = 10.17981$ Å for Y_2GaSbO_7 to $\alpha = 10.43213$ Å for Y_2InSbO_7, which indicates a decrease in the lattice parameter of the photocatalyst with a decrease of the M ionic radii, Ga^{3+} (0.62 Å) < In^{3+} (0.92 Å). The lattice parameter α also increases from $\alpha = 10.17981$ Å for Y_2GaSbO_7 to $\alpha = 10.50704$ Å for Y_2GdSbO_7, which indicates a decrease in lattice parameter of the photocatalyst with decrease of the M ionic radii, Ga^{3+} (0.62 Å) < Gd^{3+} (1.053 Å). Meanwhile, The lattice parameter α also increases from $\alpha = 10.43213$ Å for Y_2InSbO_7 to $\alpha = 10.50704$ Å for Y_2GdSbO_7, which indicates a decrease in the lattice parameter of the photocatalyst with a decrease of the M ionic radii, In^{3+} (0.92 Å) < Gd^{3+} (1.053 Å).

Figure 3 represents the diffuse reflection spectra of Y_2GaSbO_7, Y_2InSbO_7 and Y_2GdSbO_7. Compared with well-known photocatalyst TiO_2 whose absorption edge is only 380 nm, the absorption band edges of Y_2GaSbO_7, Y_2InSbO_7 and Y_2GdSbO_7 are located around 300 nm, and shoulder peaks are observed in the visible region (576 nm for Y_2GaSbO_7, 470 nm for Y_2InSbO_7, 500 nm for Y_2GdSbO_7). This is due to the formation of the impurity energy levels in the band gap of these catalysts. Clearly, the obvious absorption (defined hereby as 1-transmission) does not result from reflection and scattering. Consequently, the apparent absorbance at sub-band gap wavelengths (376 to 800 nm for Y_2GaSbO_7, and 600 to 800 nm for Y_2InSbO_7, and 550 to 800 nm for Y_2GdSbO_7) is higher than zero.

Figure 3. The diffuse reflection spectrum of Y_2GaSbO_7, Y_2InSbO_7 or Y_2GdSbO_7.

For a crystalline semiconductor, the optical absorption near the band edge follows the equation: $\alpha h v = A (h v - E_g)^n$ [20,21]. Here, A, α, E_g and v are proportional constant, absorption coefficient, band

gap and light frequency respectively. E_g and n can be calculated by the following steps: (i) plotting $\ln(\alpha h v)$ *vs.* $\ln(h v - E_g)$ by assuming an approximate value of E_g; (ii) deducing the value of n according to the slope in this graph; (iii) refining the value of E_g by plotting $(\alpha h v)^{1/n}$ *vs.* $h v$ and extrapolating the plot to $(\alpha h v)^{1/n} = 0$. According to this method, the band gap of Y_2GaSbO_7 is estimated to be 2.245 eV. The band gap of Y_2InSbO_7 is 2.618 eV and that of Y_2GdSbO_7 is 2.437 eV.

3.2. Photocatalytic Activity of Y_2GaSbO_7, Y_2InSbO_7 and Y_2GdSbO_7

Generally speaking, the semiconductor photocatalysis starts from the direct absorption of supra-band gap photons and the generation of electron–hole pairs in the semiconductor particles. Subsequently, the diffusion of the charge carriers to the surface of the semiconductor particle is followed. Under visible-light irradiation, we measured H_2 and O_2 evolution rate by using Y_2GaSbO_7, Y_2InSbO_7 and Y_2GdSbO_7 as photocatalysts from CH_3OH/H_2O and $AgNO_3/H_2O$ solutions, respectively. Wavelengths' (λ) dependence of the photocatalytic activity under light irradiation from full arc up to $\lambda = 420$ nm was measured by using different cut-off filters.

Figure 4a shows the photocatalytic H_2 evolution from pure water with Y_2GaSbO_7, Y_2InSbO_7 or Y_2GdSbO_7 as a catalyst under visible-light irradiation ($\lambda > 420$ nm, 0.5 g powder sample, 250 mL pure water). It can be found from Figure 4 that under visible-light irradiation, the rate of H_2 evolution in the first 28 h with Y_2GaSbO_7 as catalyst is 5.550 μmol h^{-1} g^{-1}, and that with Y_2InSbO_7 as catalyst is 4.764 μmol h^{-1} g^{-1}, and that with Y_2GdSbO_7 as catalyst is 3.971 μmol h^{-1} g^{-1}. The reasons that water can be split for H_2 evolution from pure water with Y_2GaSbO_7, Y_2InSbO_7 or Y_2GdSbO_7 as catalyst under visible light irradiation ($\lambda > 420$ nm) are as following: First, water can be split at a wavelength higher than 420 nm. However, the wavelength is not cut in exactly at 420 nm, in fact, the wavelength is cut by +50 or −50 nm, which means that the wavelength up to 370 nm is probably absorbed by Y_2GaSbO_7, Y_2InSbO_7 or Y_2GdSbO_7, which can split water to provide tiny amounts of hydrogen generation in our experiment. Secondly, the purchased raw materials such as Y_2O_3, Ga_2O_3 and Sb_2O_5 are mixed and synthesized together by multistep ball milling followed by ultrasonication within methanol and ethanol. As a result, the methanol or ethanol molecule will remain trapped inside Y_2GaSbO_7, Y_2InSbO_7 or Y_2GdSbO_7, even after sintering, and act as sacrificing agent to generate hydrogen from water under visible light illumination.

Three times the recycling experiments were performed with the same experimental conditions of Figure 4a, and the results were almost the same as the above results from Figure 4a. It can be seen that the photocatalysts that we have produced have recycling value.

Figure 4b shows the photocatalytic O_2 evolution from pure water with Y_2GaSbO_7, Y_2InSbO_7 or Y_2GdSbO_7 as catalyst under visible light irradiation ($\lambda > 420$ nm, 0.5 g powder sample, 250 mL pure water). It can be found from Figure 4b that under visible light irradiation, the rate of O_2 evolution in the first 28 h with Y_2GaSbO_7 as catalyst is 2.756 μmol h^{-1} g^{-1}, and that with Y_2InSbO_7 as catalyst is 2.366 μmol h^{-1} g^{-1}, and that with Y_2GdSbO_7 as catalyst is 1.966 μmol h^{-1} g^{-1}.

Figure 4c shows the photocatalytic H_2 evolution from aqueous methanol solution with Y_2GaSbO_7, Y_2InSbO_7 or Y_2GdSbO_7 as catalyst under visible light irradiation ($\lambda > 420$ nm, 0.5 g 0.1wt % Pt-loaded powder sample, 50 mL methanol solution, 200 mL pure water). It can be found from Figure 4c that under visible light irradiation, the rate of H_2 evolution in the first 28 h with Y_2GaSbO_7 as catalyst is

16.657 μmol h^{-1} g^{-1}, and that with Y_2InSbO_7 as catalyst is 11.843 μmol h^{-1} g^{-1}, and that with Y_2GdSbO_7 as catalyst is 10.307 μmol h^{-1} g^{-1}, indicating that the photocatalytic activity of Y_2GaSbO_7 is much higher than that of Y_2InSbO_7 or Y_2GdSbO_7.

Figure 4. (**a**) Photocatalytic H_2 evolution and (**b**) photocatalytic O_2 evolution from pure water with Y_2GaSbO_7, Y_2InSbO_7 or Y_2GdSbO_7 as catalyst under visible light irradiation (λ > 420 nm, 0.5 g powder sample, 250 mL pure water). Light source: 300 W Xe lamp. (**c**) Photocatalytic H_2 evolution from aqueous methanol solution with Y_2GaSbO_7, Y_2InSbO_7 or Y_2GdSbO_7 as catalyst under visible light irradiation (λ > 420 nm, 0.5 g 0.1 wt % Pt-loaded powder sample, 50 mL methanol solution, 200 mL pure water). Light source: 300 W Xe lamp.
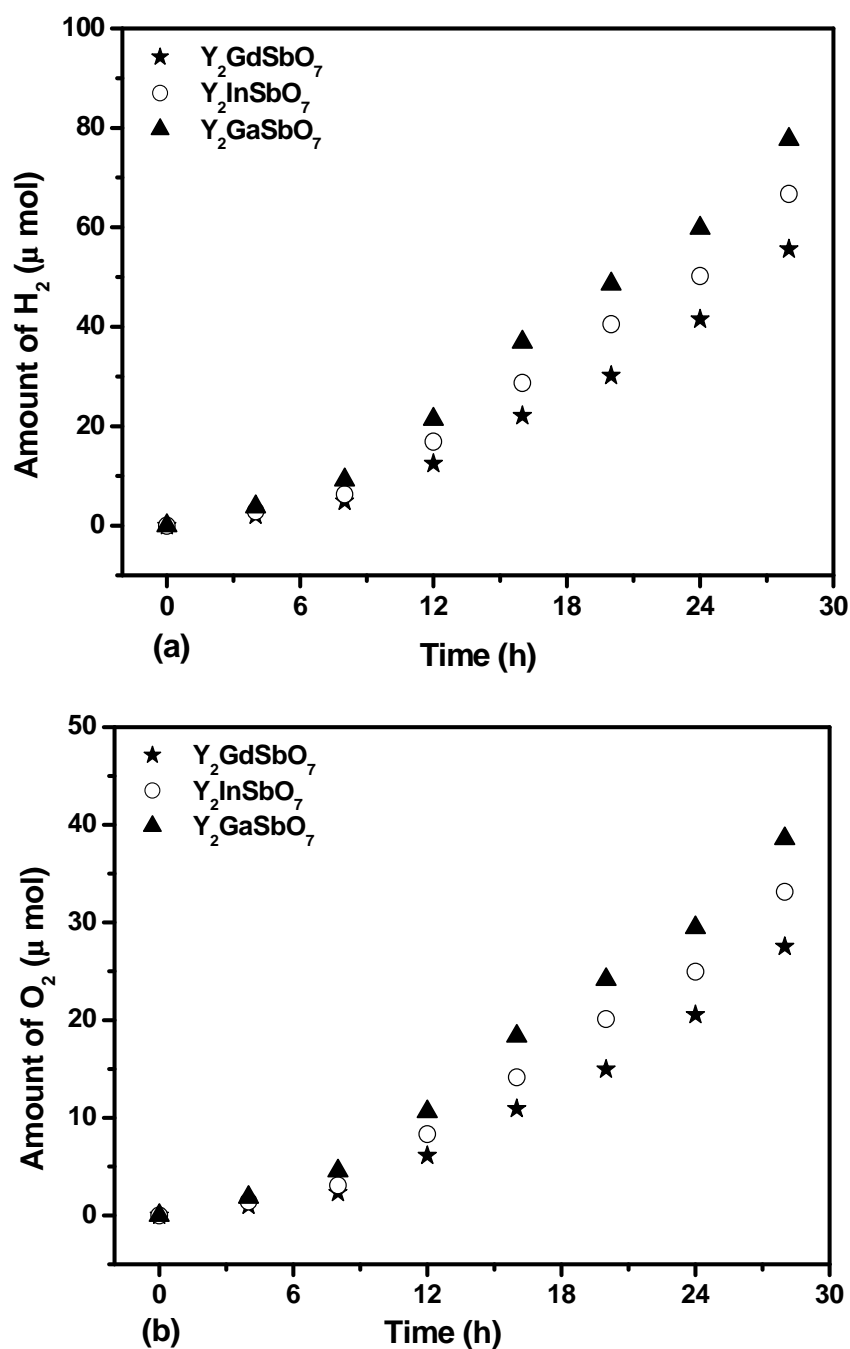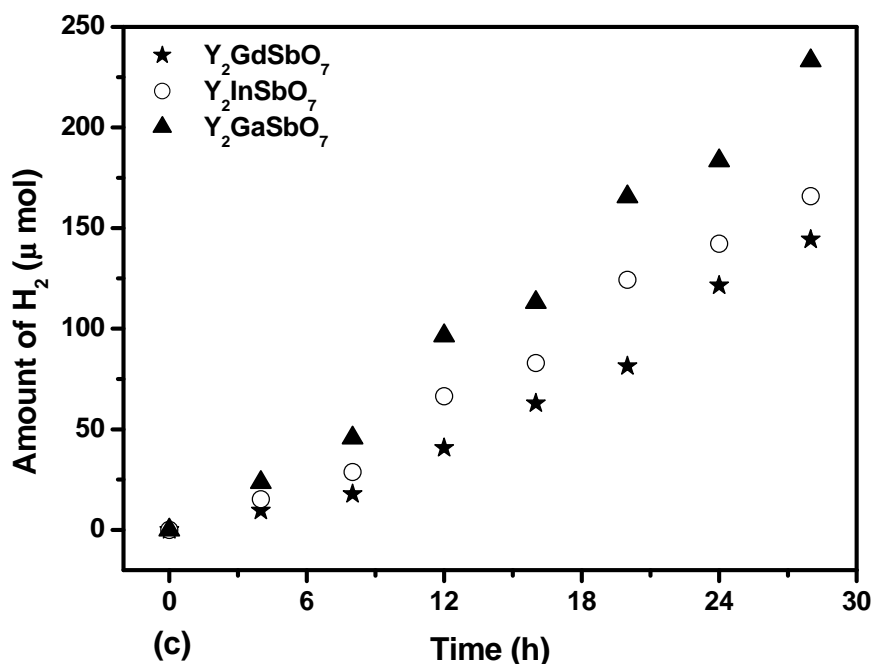
Figure 4. *Cont.*

(c)

We will estimate apparent quantum yield in this paper because scattering effects are assumed to be the same for all the photocatalysts and our system is a suspension rather than a homogeneous solution. The apparent quantum yield for hydrogen evolution at 420 nm with Y_2GaSbO_7 as catalyst is 0.407%, and that with Y_2InSbO_7 as catalyst is 0.289% and that with Y_2GdSbO_7 as catalyst is 0.252% under visible light irradiation. Moreover, Y_2InSbO_7 shows higher photocatalytic activity than Y_2GdSbO_7. This also proves that the conduction band level of Y_2GaSbO_7, Y_2InSbO_7 or Y_2GdSbO_7 is more negative than the reduction potential of H_2O for forming H_2. The formation rate of H_2 increased with decreasing the M ionic radii within Y_2MSbO_7 (M = Ga, In, Gd), Ga^{3+} (0.62 Å) < In^{3+} (0.92 Å) < Gd^{3+} (1.053 Å). The reason is that the surface area of the photocatalyst increases with decreasing the M ionic radii, and the creation of more active sites is realized; as a result, the hydrogen generation rate increases. Moreover, the decrease of the M ionic radii will result in a decrease for the migration distance of photogenerated electrons and holes to reach the reaction site on the photocatalyst surface. Thus the photogenerated electrons and holes can get to the photocatalyst surface more quickly. The above factors will suppress the electron–hole recombination and, therefore, the photocatalytic activity will be enhanced. Such results are in good agreement with the optical absorption property of Y_2GaSbO_7, Y_2InSbO_7 or Y_2GdSbO_7 (see Figure 3). The rate of H_2 evolution also increases with increasing illumination time. The photocatalytic activity of Y_2GaSbO_7 increases by about 162% than that of Y_2GdSbO_7.

Figure 5 shows the photocatalytic O_2 evolution from $AgNO_3$ solution with Y_2GaSbO_7, Y_2InSbO_7 or Y_2GdSbO_7 as catalyst under visible light irradiation ($\lambda > 420$ nm, 0.5 g photocatalyst, 1 mmol $AgNO_3$, 270 mL pure water). It can be seen from Figure 5 that under visible light irradiation, the rate of O_2 evolution in the first 28 h with Y_2GaSbO_7 as catalyst is 33.779 µmol h^{-1} g^{-1}, and that with Y_2InSbO_7 as catalyst is 22.314 µmol h^{-1} g^{-1}, and that with Y_2GdSbO_7 as catalyst is 16.393 µmol h^{-1} g^{-1}, indicating that the valence band level of Y_2GaSbO_7, Y_2InSbO_7 or Y_2GdSbO_7 is more positive than the

oxidation potential of H_2O for forming O_2. The formation rate of O_2 increases with decreasing the M ionic radii within Y_2MSbO_7 (M = Ga, In, Gd), Ga^{3+} (0.62 Å) < In^{3+} (0.92 Å) < Gd^{3+} (1.053 Å). The formation rate of O_2 increased by decreasing the M ionic radii within Y_2MSbO_7 (M = Ga, In, Gd), Ga^{3+} (0.62 Å) < In^{3+} (0.92 Å) < Gd^{3+} (1.053 Å). The reason is that the surface area of the photocatalyst increases with the decrease in the M ionic radii, and the creation of more active sites is realized. As a result, the oxygen generation rate increases. Moreover, the decrease of the M ionic radii will result in a decrease of the migration distance of photogenerated electrons and holes to reach the reaction site on the photocatalyst surface. Thus, the photogenerated electrons and holes can get to the photocatalyst surface more quickly. Above factors will suppress the electron–hole recombination and therefore the O_2 evolution rate increases by decreasing the M ionic radii within Y_2MSbO_7 (M = Ga, In, Gd). The apparent quantum yield for the oxygen evolution at 420 nm with Y_2GaSbO_7 as catalyst is 1.650%, and that with Y_2InSbO_7 as catalyst is 1.090%, and that with Y_2GdSbO_7 as catalyst is 0.801% under visible light irradiation.

Figure 5. Photocatalytic O_2 evolution from $AgNO_3$ solution with Y_2GaSbO_7, Y_2InSbO_7 or Y_2GdSbO_7 as catalyst under visible light irradiation (λ > 420 nm, 0.5 g photocatalyst, 1 mmol $AgNO_3$, 270 mL pure water). Light source: 300 W Xe lamp.
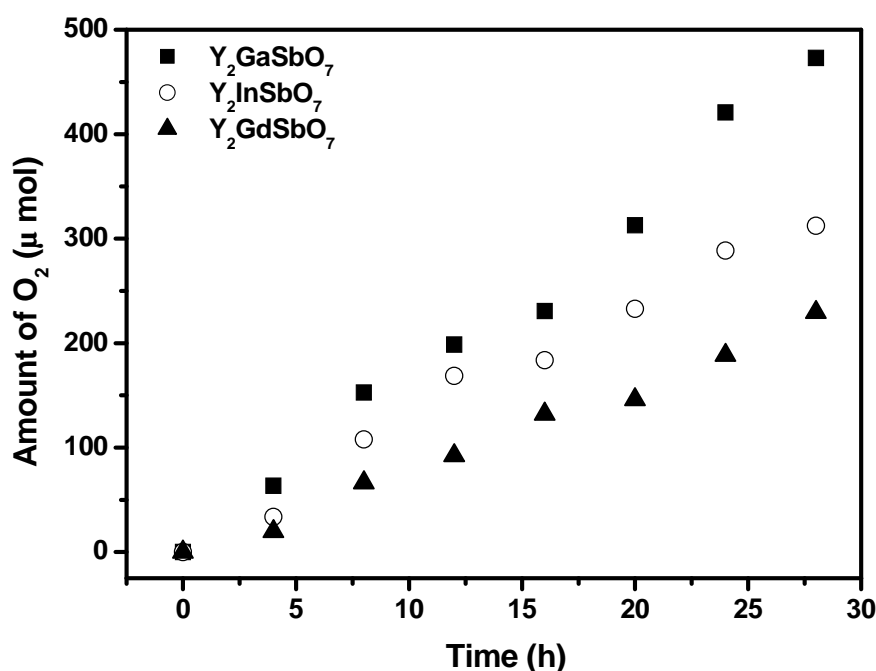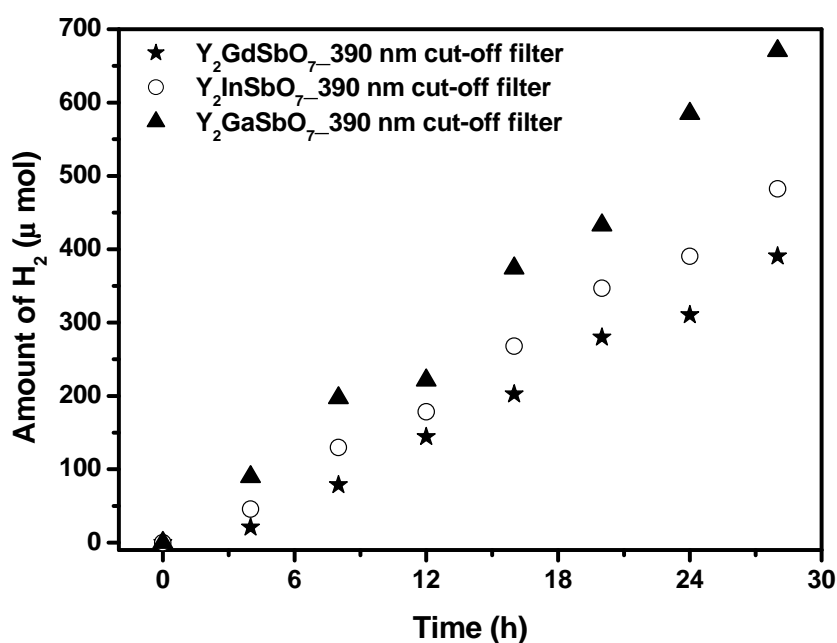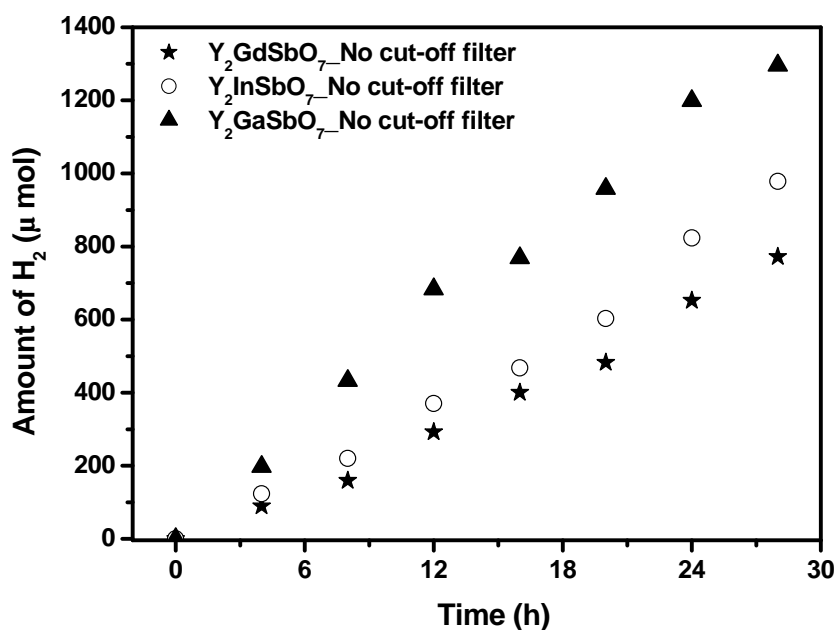

Figure 6 shows the photocatalytic H_2 evolution from aqueous methanol solution with Y_2GaSbO_7, Y_2InSbO_7 or Y_2GdSbO_7 as catalyst under light irradiation (390 nm cut-off filter, 0.5 g 0.1 wt % Pt-loaded powder sample, 50 mL CH_3OH, 200 mL pure water). It is depicted in Figure 6 that under light irradiation (390 nm cut-off filter), the rate of H_2 evolution in the first 28 h with Y_2GaSbO_7 as catalyst is 47.900 μmol h^{-1} g^{-1}, and that with Y_2InSbO_7 as catalyst is 34.450 μmol h^{-1} g^{-1}, and that with Y_2GdSbO_7 as catalyst is 27.893 μmol h^{-1} g^{-1}, indicating that the effect of wavelength (λ) dependence on the photocatalytic activity is very important. The formation rate of H_2 increased with decreasing the M ionic radii within Y_2MSbO_7 (M = Ga, In, Gd), Ga^{3+} (0.62 Å) < In^{3+} (0.92 Å) < Gd^{3+} (1.053 Å). As the M ionic radii decreases, the surface area of the photocatalyst increases. Subsequently, more active

sites appear, and, at the same time, the decrease of the M ionic radii causes a decrease for the migration distance of photogenerated electrons and holes to reach the reaction site of the photocatalyst surface, thus hydrogen generation rate increases with decreasing the M ionic radii within Y_2MSbO_7 (M = Ga, In, Gd). The apparent quantum yield for hydrogen evolution at 390 nm with Y_2GaSbO_7 as catalyst is 1.170%, and that with Y_2InSbO_7 as catalyst is 0.841% and that with Y_2GdSbO_7 as catalyst is 0.681% under light irradiation (390 nm cut-off filter).

Figure 6. Photocatalytic H_2 evolution from aqueous methanol solution with Y_2GaSbO_7, Y_2InSbO_7 or Y_2GdSbO_7 as catalyst under light irradiation (390 nm cut-off filter, 0.5 g 0.1 wt % Pt-loaded powder sample, 50 mL CH_3OH, 200 mL pure water). Light source: 300 W Xe lamp.

The photocatalytic H_2 evolution from aqueous methanol solution with Y_2GaSbO_7, Y_2InSbO_7 or Y_2GdSbO_7 as catalyst under light irradiation (No cut-off filter, 0.5 g 0.1 wt % Pt-loaded powder sample, 50 mL CH_3OH, 200 mL pure water) are shown in Figure 7. It can be found from Figure 7 that under light irradiation without using any filters, the rate of H_2 evolution in the first 28 h with Y_2GaSbO_7 as catalyst is 92.543 μmol h^{-1} g^{-1}, and that with Y_2InSbO_7 as catalyst is 69.886 μmol h^{-1} g^{-1}, and that with Y_2GdSbO_7 as catalyst is 55.157 μmol h^{-1} g^{-1}, indicating that Y_2GaSbO_7, Y_2InSbO_7 or Y_2GdSbO_7 shows high photocatalytic activity under full arc irradiation. The apparent quantum yield for hydrogen evolution at 420 nm with Y_2GaSbO_7 as catalyst is 2.260%, and that with Y_2InSbO_7 as catalyst is 1.707%, and that with Y_2GdSbO_7 as catalyst is 1.347% under light irradiation without using any filters. The photocatalytic activity decreases with increasing incident wavelength λ. As to Y_2GaSbO_7, Y_2InSbO_7 or Y_2GdSbO_7, the turnover number—the ratio of total amount of gas evolves to catalyst—exceeded 0.224 for Y_2GaSbO_7, 0.175 for Y_2InSbO_7, and 0.164 for Y_2GdSbO_7, respectively after 28 h of reaction time under visible light irradiation ($\lambda > 420$ nm). The turnover number is in terms of reacted electrons relative to the amount of Y_2GaSbO_7 reaching 1 at 55 h reaction time. As for Y_2InSbO_7, the turnover number exceeds 1 after 68 h reaction time. As to Y_2GdSbO_7, the turnover

number exceeds 1 after 76 h reaction time. Under the condition of full arc irradiation, after 28 h of reaction time, the turnover number exceeds 1.247 for Y_2GaSbO_7, and the turnover number exceeds 1.030 for Y_2InSbO_7, and the turnover number exceeds 0.878 as to Y_2GdSbO_7. The above results are enough to prove that the reaction occurred catalytically. The reaction stopped when the light was turned off in this experiment, showing the obvious light response.

Figure 7. Photocatalytic H_2 evolution from aqueous methanol solution with Y_2GaSbO_7, Y_2InSbO_7 or Y_2GdSbO_7 as catalyst under light irradiation (No cut-off filter, 0.5 g 0.1 wt % Pt-loaded powder sample, 50 mL CH_3OH, 200 mL pure water). Light source: 300 W Xe lamp.
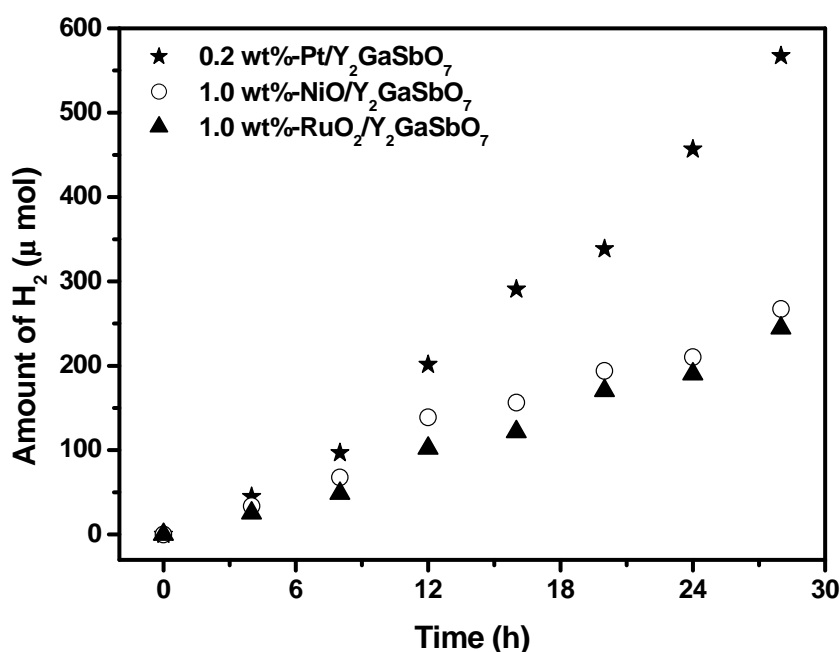

It was known that TiO_2 has very high photocatalytic activity under ultraviolet light irradiation. By contrast, the photocatalytic activity was not obtained with Pt/TiO_2 as catalyst under visible light irradiation ($\lambda > 420$ nm), while an obvious photocatalytic activity was observed with Y_2GaSbO_7, Y_2InSbO_7 or Y_2GdSbO_7 as catalyst, showing that Y_2GaSbO_7, Y_2InSbO_7 or Y_2GdSbO_7 can respond to visible light irradiation. The formation rate of H_2 evolution with Y_2GaSbO_7, Y_2InSbO_7 or Y_2GdSbO_7 as catalyst was much larger than that with TiO_2 as catalyst under visible light irradiation. This indicated that the photocatalytic activity of Y_2GaSbO_7, Y_2InSbO_7 or Y_2GdSbO_7 for decomposing CH_3OH/H_2O solution was higher than that of TiO_2. The structure of Y_2GaSbO_7, Y_2InSbO_7 or Y_2GdSbO_7 after photocatalytic reaction was also checked by using X-ray diffraction method, and no change in their structures were observed during this reaction, which indicated that the H_2 evolution was resulted from the photocatalytic reaction of H_2O. SEM-EDS results also confirmed that the chemical composition of Y_2GaSbO_7, Y_2InSbO_7 or Y_2GdSbO_7 did not change after reaction.

Figure 8 shows the effect of Pt, NiO and RuO_2 co-catalysts on the photoactivity of Y_2GaSbO_7 under visible light irradiation ($\lambda > 420$ nm, 0.5 g powder sample, 50 mL methanol solution, 200 mL pure water). In principle, the photoinduced electrons preferentially enriched on the surface of co-catalyst particles and the recombination of the photoinduced electrons with the photoinduced holes were therefore markedly suppressed. It can be found from Figure 8 that in the first 28 h under visible light

irradiation, the rate of H_2 evolution is estimated to be 40.529 µmol h^{-1} g^{-1} with 0.2 wt %-Pt/ Y_2GaSbO_7 as catalyst, and that is estimated to be 19.100 µmol h^{-1} g^{-1} with 1.0 wt %-NiO/Y_2GaSbO_7 as catalyst, and that is estimated to be 17.486 µmol h^{-1} g^{-1} with 1.0 wt %-RuO$_2$/Y_2GaSbO_7 as catalyst, indicating that the photocatalytic activities can be further improved under visible light irradiation with Y_2GaSbO_7, Y_2InSbO_7 or Y_2GdSbO_7 being loaded by Pt, NiO or RuO$_2$. The apparent quantum yield for hydrogen evolution at 420 nm with 0.2 wt %-Pt/Y_2GaSbO_7 as catalyst is 0.990%, and that with 1.0 wt %-NiO/Y_2GaSbO_7 as catalyst is 0.466%, and that with 1.0 wt %-RuO$_2$/Y_2GaSbO_7 as catalyst, is 0.427% under visible light irradiation ($\lambda > 420$ nm). The effect of Pt is better than that of NiO or RuO$_2$ for improving the photocatalytic activity of Y_2GaSbO_7, Y_2InSbO_7 or Y_2GdSbO_7.

Figure 8. Effect of Pt, NiO and RuO$_2$ co-catalysts on the photoactivity of Y_2GaSbO_7 under visible light irradiation ($\lambda > 420$ nm, 0.5 g powder sample, 50 mL methanol solution, 200 mL pure water). Light source: 300 W Xe lamp.

It is known that the process for photocatalysis of semiconductors is the direct absorption of photon by band gap of the materials and generates electron–hole pairs in the semiconductor particles, and the excitation of an electron from the valence band to the conduction band is initiated by light absorption with energy equal to or greater than the band gap of the semiconductor. Upon excitation of photon, the separated electron and hole can follow the solid surface. This suggests that the narrow band gap was easier to excite an electron from the valence band to the conduction band. If the conduction band potential level of the semiconductor is more negative than that of H_2 evolution, and the valence band potential level is more positive than that of O_2 evolution, decomposition of water can occur even without applying electric power [1]. According to the above analysis, the photon absorption of Y_2GaSbO_7 is much easier than that of the Y_2InSbO_7 or Y_2GdSbO_7, which results in higher photocatalytic activity of Y_2GaSbO_7.

The specific surface area of Y_2GaSbO_7 is measured to be 3.84 m^2/g which is about 7.138% of the surface area of the TiO$_2$ photocatalyst (53.8 m^2 g^{-1}), and the surface area of Y_2InSbO_7 is measured to

be 1.76 $m^2 g^{-1}$, which is only about 3.271% of the surface area of TiO_2, and the specific surface area of Y_2GdSbO_7 is measured to be 1.61 $m^2 g^{-1}$ which is only about 2.993% of the surface area of TiO_2. It indicates much higher potential efficiency of Y_2GaSbO_7, Y_2InSbO_7 or Y_2GdSbO_7. Although the surface area of Y_2GaSbO_7, Y_2InSbO_7 or Y_2GdSbO_7 is smaller than that of TiO_2, but Y_2GaSbO_7, Y_2InSbO_7 or Y_2GdSbO_7 shows higher photocatalytic activity for H_2 evolution under visible light irradiation, which indicates that the high photocatalytic activity of the Y_2GaSbO_7, Y_2InSbO_7 or Y_2GdSbO_7 is not owing to a big surface area, but rather owing to the narrow band gap. It is obvious that further increase in photocatalytic activity might be prospected from increasing the surface area of Y_2GaSbO_7, Y_2InSbO_7 or Y_2GdSbO_7. Since an efficient photocatalytic reaction process occurred on the photocatalyst surface, the increase of the surface area for the photocatalysts might lead to the increase of their photocatalytic activity.

4. Conclusions

In the present work, we prepared single phase of Y_2GaSbO_7, Y_2InSbO_7 or Y_2GdSbO_7 by solid-state reaction method and studied the structural, optical and photocatalytic properties of Y_2GaSbO_7, Y_2InSbO_7 or Y_2GdSbO_7. Rietveld structure refinement reveals that Y_2GaSbO_7, Y_2InSbO_7 or Y_2GdSbO_7 crystallized with the pyrochlore-type structure, cubic crystal system and space group *Fd3m*. The lattice parameter for Y_2GaSbO_7 is 10.17981 Å. The lattice parameter for Y_2InSbO_7 is 10.43213 Å. The lattice parameter for Y_2GdSbO_7 is 10.50704 Å. The band gap of Y_2GaSbO_7 is estimated to be 2.245 eV. The band gap of Y_2InSbO_7 is 2.618 eV. The band gap of Y_2GdSbO_7 is 2.437 eV. Y_2GaSbO_7, Y_2InSbO_7 or Y_2GdSbO_7 shows optical absorption in the visible light region, indicating that the photocatalysts have the ability to respond to the wavelength of visible light region. For the photocatalytic water-splitting reaction, H_2 or O_2 evolution is observed from pure water with Y_2GaSbO_7, Y_2InSbO_7 or Y_2GdSbO_7 as catalyst under visible light irradiation ($\lambda > 420$ nm). In addition, under visible light irradiation ($\lambda > 420$ nm), H_2 and O_2 are also evolved by using Y_2GaSbO_7, Y_2InSbO_7 or Y_2GdSbO_7 as catalyst from CH_3OH/H_2O and $AgNO_3/H_2O$ solutions, respectively. Y_2GaSbO_7 shows the highest activity compared with Y_2InSbO_7 or Y_2GdSbO_7. At the same time, Y_2InSbO_7 shows higher activity compared with Y_2GdSbO_7. The photocatalytic activities are further improved under visible light irradiation with Y_2GaSbO_7, Y_2InSbO_7 or Y_2GdSbO_7 being loaded by Pt, NiO or RuO_2. The effect of Pt is better than that of NiO or RuO_2 for improving the photocatalytic activity of Y_2GaSbO_7, Y_2InSbO_7 or Y_2GdSbO_7. Moreover, the synthesis of Y_2GaSbO_7, Y_2InSbO_7 or Y_2GdSbO_7 offers some useful insights for the design of new photocatalysts for the photocatalytic evolution of H_2 and O_2.

References

1. Fujishima, A.; Honda, K. Electrochemical photolysis of water at a semiconductor electrode. *Nature* **1972**, *238*, 37–38.

2. Neppolian, B.; Yamashita, H.; Okada, Y.; Nishijima, H.; Anpo, M. Preparation of unique TiO_2 nano-particle photocatalysts by a multi-gelation method for control of the physicochemical parameters and reactivity. *Catal. Lett.* **2005**, *105*, 111–117.

3. Takeuchi, M.; Sakamoto, K.; Martra, G.; Coluccia, S.; Anpo, M. Mechanism of photoinduced superhydrophilicity on the TiO_2 photocatalyst surface. *J. Phys. Chem. B* **2005**, *109*, 15422–15428.

4. Chen, H.N.; Li, W.P.; Liu, H.C.; Zhu, L.Q. Performance enhancement of CdS-sensitized TiO_2 mesoporous electrode with two different sizes of CdS nanoparticles. *Microporous Mesoporous Mater.* **2011**, *138*, 235–238.

5. Zou, Z.; Ye, J.; Sayama, K.; Arakawa, H. Direct splitting of water under visible light irradiation with an oxide semiconductor photocatalyst. *Nature* **2001**, *414*, 625–627.

6. Zou, Z.; Ye, J.; Arakawa, H. Surface characterization of nanoparticles of $NiO_x/In_{0.9}Ni_{0.1}TaO_4$: Effects on photocatalytic activity. *J. Phys. Chem. B* **2002**, *106*, 13098–13101.

7. Zou, Z.; Ye, J.; Arakawa, H. Preparation, structural and photophysical properties of Bi_2InNbO_7 compound. *J. Mater. Sci. Lett.* **2000**, *19*, 1909–1911.

8. Anpo, M.; Takeuchi, M. The design and development of highly reactive titanium oxide photocatalysts operating under visible light irradiation. *J. Catal.* **2003**, *19*, 505–516.

9. Malato, S.; Blanco, J.; Cáceres, J.; Fernández-alba, A.R.; Agüera, A.; Rodríguez, A. Photocatalytic treatment of water-soluble pesticides by photo-Fenton and TiO_2 using solar energy. *Catal. Today* **2002**, *76*, 209–220.

10. Kodama, T.; Isobe, Y.; Kondoh, Y.; Yamaguchi, S.; Shimizu, K.I. Ni/ceramic/molten-salt composite catalyst with high-temperature thermal storage for use in solar reforming processes. *Energy* **2004**, *29*, 895–903.

11. Guan, G.; Kida, T.; Yoshida, A. Reduction of carbon dioxide with water under concentrated sunlight using photocatalyst combined with Fe-based catalyst. *Appl. Catal. B Environ.* **2003**, *41*, 387–396.

12. Guan, G.; Kida, T.; Harada, T.; Isayama, M.; Yoshida, A. Photoreduction of carbon dioxide with water over $K_2Ti_6O_{13}$ photocatalyst combined with Cu/ZnO catalyst under concentrated sunlight. *Appl. Catal. A Gen.* **2003**, *249*, 11–18.

13. Nann, T.; Ibrahim, S.K.; Woi, P.M.; Xu, S.; Ziegler, J.; Pickett, C.J. Water splitting by visible light: A nanophotocathode for hydrogen production. *Angew. Chem. Int. Ed.* **2010**, *49*, 1574–1577.

14. Luan, J.; Cai, H.; Zheng, S.; Hao, X.; Luan, G.; Wu, X.; Zou, Z. Structural and photocatalytic properties of novel Bi_2GaVO_7. *Mater. Chem. Phys.* **2007**, *104*, 119–124.

15. Luan, J.; Hao, X.; Zheng, S.; Luan, G.; Wu, X. Structural, photophysical and photocatalytic properties of Bi_2MTaO_7 (M = La and Y). *J. Mater. Sci.* **2006**, *41*, 8001–8012.

16. Huang, Y.; Zheng, Z.; Ai, Z.; Zhang, L.; Fan, X.; Zou, Z. Core-shell microspherical $Ti_{1-x}Zr_xO_2$ solid solution photocatalysts directly from ultrasonic spray pyrolysis. *J. Phys. Chem. B.* **2006**, *110*, 19323–19328.

17. Borse, P.; Joshi, U.; Ji, S.; Jang, J.; Lee, J.; Jeong, E.; Kim, H. Band gap tuning of lead-substituted BaSnO3 for visible light photocatalysis. *Appl. Phys. Lett.* **2007**, *90*, 034103:1–034103:3.

18. Yi, Z.; Ye, J. Band gap tuning of $Na_{1-x}La_xTa_{1-x}Co_xO_3$ solid solutions for visible light photocatalysis. *Appl. Phys. Lett.* **2007**, *91*, 254108:1–254108:3.

19. Tang, J.; Zou, Z.; Yin, J.; Ye, J. Structural, Photocatalytic degradation of methylene blue on $CaIn_2O_4$ under visible light irradiation. *Chem. Phys. Lett.* **2003**, *382*, 175–179.

20. Tauc, J.; Grigorovici, R.; Vancu, A. Optical properties and electronic strcuture of amorphous germanium. *Phys. Status Solid* **1966**, *15*, 627–637.

21. Butler, M. Photoelectrolysis and physical-properties of semiconducting electrode WO_3. *J. Appl. Phys.* **1977**, *48*, 1914–1920.